Chinese Chemical Letters 35 (2024) 109573

Contents lists available at ScienceDirect

Chinese Chemical Letters

journal homepage: www.elsevier.com/locate/cclet

Designing unimolecular photoinitiator by installing NHPI esters along the TX backbone for acrylate photopolymerization and their applications in coatings and 3D printing

Yi Zhu [a,b], Jingyan Zhang [b], Yuchao Zhang [d], Ying Chen [b], Guanghui An [c,*], Ren Liu [a,b,*]

[a] Key Laboratory of Synthetic and Biological Colloids, Ministry of Education, School of Chemical and Material Engineering, Jiangnan University, Wuxi 214122, China
[b] International Research Center for Photoresponsive Molecules and Materials, Jiangnan University, Wuxi 214122, China
[c] School of Chemistry and Materials Science, Heilongjiang University, Harbin 150080, China
[d] Scientific Experiment Center, Hangzhou Institute of Medicine (HIM), Chinese Academy of Sciences, Hangzhou 310022, China

ARTICLE INFO

Article history:
Received 8 November 2023
Revised 19 January 2024
Accepted 23 January 2024
Available online 29 January 2024

Keywords:
Photopolymerization
Photoinitiator
Energy transfer
Thioxanthone
N-Hydroxyphthalimide ester

ABSTRACT

Developing efficient and long wavelength sensitive unimolecular photoinitiators (PIs) is still facing a great challenge. In this work, a series of thioxanthone-based *N*-hydroxyphthalimide esters (TX-NHPIEs) were synthesized by installing NHPIEs along the TX backbone and characterized. The investigated TX-NHPIEs have a 60 nm redshift and demonstrate sterling initiating efficiency for free radical photopolymerization (FRP) under LED@450 nm light irradiation compared with the commercialized isopropylthioxanthone (ITX). Real-time ^{1}Hnuclear magnetic resonance (^{1}H NMR), electron spin resonance (ESR), decarboxylation and gas chromatograph-mass spectrometer (GC–MS) experiments and density functional theory (DFT) reveal that TX-NHPIEs can generate one alkyl radical and one N-centered iminyl radical, which can initiate FRP directly and indirectly, respectively. In other words, TX-NHPIEs absorb one photon and can generate two active radicals, which break through the limitations of common PIs. TX-NHPIE-Cpe demonstrates the highest initiating efficiency, and its application in coatings and 3D printing was also studied, indicating TX-NHPIEs have broad potential applications in photopolymerization processes.

With the advantages of green efficiency and spatiotemporal control, photopolymerization has been a promising method for synthesizing desired macromolecules [1–4]. The successful applications on coatings [5–7], printing inks [8,9], electronic circuits [10,11], digital storage [12,13], solar cell [14], additive manufacturing [15–19] and dental materials [20] demonstrate the advanced and practical nature of photopolymerization. As the central part of photopolymerization, photoinitiators (PIs) determine the type of irradiation light sources, the speed and type of photopolymerization and affect the performance of photopolymerisable materials [21,22]. As we know, the absorption of most reported high-efficiency PIs is in the ultraviolet (UV) and far ultraviolet regions, making UV mercury lamps the most common traditional photopolymerization irradiation source [23]. However, issues such as ozone, excess heat and light pollution will arise in photopolymerization [24]. Thus, developing PIs with high initiating efficiency, excellent photochemical and photophysical properties, and long wavelength sensitivity which match the emission wavelength of light-emitting diodes (LEDs) have become an attractive research direction [25,26].

LEDs have obtained comprehensive development, attributed to the advantages of portability, low heat generation, high safety, low energy consumption, low cost, and so on, in various fields recently [27]. However, the application of most commercial PIs in photopolymerization initiated by LED lamps is restricted, because LED lights have a very narrow emission bandwidth at long wavelength [28]. Currently, the design and development of highly active PIs that match the emission spectrum of LED light sources is the main research direction in the field of photopolymerization, especially the development of 450 nm absorbable PIs. The development of bi-component and multi-component irradiation systems, such as thioxanthone (TX) derivatives combined with onium salt, amine, and other additives, is the general strategy to match the emission spectrum of LED light sources. However, irritating smell, toxicity, yellowing, solubility, compatibility, migration, and initiating efficiency are affected by electron transfer efficiency reduced when the photopolymerization system gradually becomes viscous

* Corresponding authors.
E-mail addresses: chemagh@163.com (G. An), liuren@jiangnan.edu.cn (R. Liu).

https://doi.org/10.1016/j.cclet.2024.109573
1001-8417/

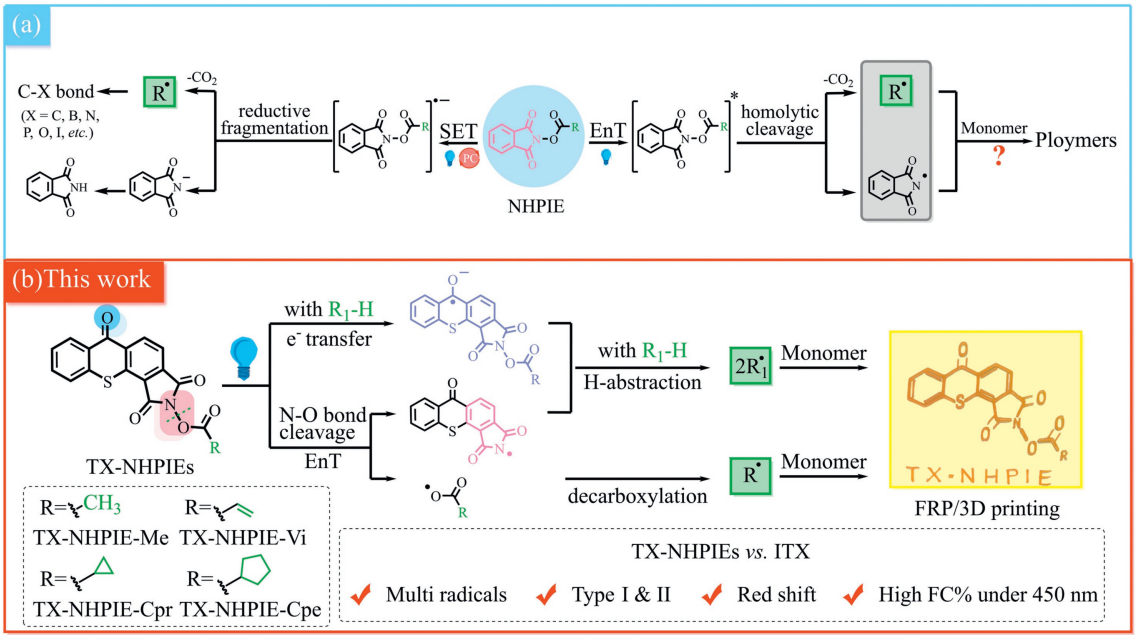

Fig. 1. Schematic diagram of the previous related work and this work.

[29], making bi-component and multi-component systems less attractive for industrial applications.

Unlike bi-component and multi-component systems, unimolecular PIs absorb light energy and directly undergo homolytic or heterolytic cleavage to produce active species that initiate polymerization [30]. The most prevalent approach to enhance the absorption range of PIs is to incorporate auxochromic or conjugated groups into the molecular backbone. Nevertheless, introducing and extending the conjugation system leads to a diminished energy gap between the lowest unoccupied molecular orbital (LUMO) and highest occupied molecular orbital (HOMO), which causes a crossover between the σ^* and π^* LUMO states [31], which results in the decline of the desired bonds cleavage efficiency. An excellent strategy for solving these problems is to install weak chemical bonds in PIs, such as N–O bonds in redox active esters (RAEs). Our group [32] developed a series of coumarin-based oxime ester PIs (N–O bond energy = 60.34–64.78 kcal/mol) with good initiation efficiency. Lalevée *et al.* [33] researched a series of nitro carbazole-based oxime ester PIs (N–O bond energy = 44.16–46.21 kcal/mol) which have excellent light absorption properties and photoinitiation abilities in the visible range. Shortly afterward, Lalevée *et al.* [34] synthesized and studied *N*-naphthalimide esters (N–O bond energy = 61.41-63.17 kcal/mol) as type I PIs for FRP. However, only one active radical can be produced after RAEs absorb one photon, while imine radicals have no initiating activity and tend to dimerize or extract hydrogen atoms from the solvent or be oxidized to aldehydes [35]. Therefore, designing and synthesizing a PI that can produce two or more active radicals after absorbing one photon will enhance the utilization efficiency of the photon. As a classic RAE, NHPIE mainly through a single electron transfer (SET) process to construct C-X bonds (X = C, B, N, P, O, I, *etc.*) (Fig. 1) under the conditions of corresponding photo-catalysts [36–39]. It is worth noting that only C radical can be used to form the desired chemical bonds, but the phthalimidyl anion is mostly not utilized resulting in atomic waste, in the SET process. Thus, developing a novel NHPIE, which can generate two usable free radicals under light irradiation *via* an energy transfer (EnT) mechanism, will greatly improve the utilization efficiency of photons and the application range of NHPIE.

TX derivatives as bi-component and multi-component initiating systems have been successfully applied in the field of photopolymerization, because of the properties of low triplet energy, high quantum yield and excellent absorption performance from 360 nm to 420 nm [40,41]. Although the TX system has been commercialized, it also has the shortcomings of a bi-component or multi-component system [42]. Therefore, it is necessary to study the unimolecular PIs based on the TX skeleton. Herein, we designed and synthesized a series of novel unimolecular and long wavelength sensitive PIs, which absorb one photon and can produce two active radicals through the process of EnT, by installing NHPIEs along the TX backbone (Fig. 1). The absorption of the obtained TX-NHPIEs redshift 60 nm compared with the commercialized ITX. The obtained TX-NHPIEs not only can act as unimolecular PI, but also can act as a bi-component initiate system for FRP. The influence of different ester groups on photoinitiated activity was elucidated. Real-time ^{1}Hnuclear magnetic resonance (^{1}H NMR), electron spin resonance (ESR), decarboxylation and gas chromatograph-mass spectrometer (GC–MS) experiments and computational studies have confirmed the EnT mechanism. The applications of TX-NHPIE-Cpe in coatings and 3D printing were also studied. It is anticipated that our work breaks through the limitations of common PIs and provides certain guidance for the design of new high-efficiency PIs.

As shown in Fig. 2a and Table S1 (Supporting information), four kinds of TX-NHPIEs have similar absorption spectra and photophysical properties, and the maximum absorption peaks of TX-NHPIEs all at 284 nm and 422 nm, which can be attributed to the fact that they have the same backbone and the terminal alkyl groups do not participate in conjugation. Notably, TX-NHPIEs have a wide absorption from 250 nm to 480 nm, and the maximum absorption wavelength shifts to 480 nm, which is much longer than ITX. These properties give TX-NHPIEs the possibility to initiate FRP under the commercial UV and visible LED light sources. Density functional theory (DFT) calculation [43] indicates that experimental results are consistent with the DFT calculation results (Fig. 2b), which all confirm the excellent optical absorption of TX-NHPIEs. The fluorescence emission spectra of TX-NHPIEs exhibit a consistent pattern, with fluorescence emission wavelength ranging from 430 nm to 680 nm (Fig. S1 in Supporting information). By analyzing natu-

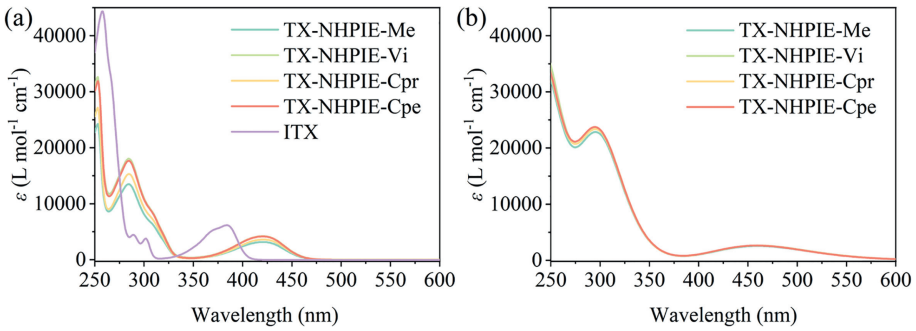

Fig. 2. UV–vis absorption spectra (experimental (a) and computational (b)) of ITX and TX-NHPIEs in CH_3CN at ambient temperature ([PI] = 5.0×10^{-5} mol/L). The first 30 singlet excited states computed through the B3LYP/6-311G** (CH_3CN) level.

ral transition orbitals (NTO), it is possible to classify the type of transition in the singlet excited state (S_1) in TX-NHPIEs as a typical charge transfer π-π^* excitation. Both occupied and virtual NTO pairs are located on thioxanthone-based phthalimide (TX-PI) fragments regardless of the substituent groups (Table S2 in Supporting information), which indicates that the introduction of different substituents has a negligible effect on the maximum wavelength because of the similarity of π-electron delocalization in these structures [44].

Photolysis experiments of four TX-NHPIEs and ITX were carried out under the irradiation of LED@365, 405 and 450 nm light sources, respectively. As shown in Fig. S2 (Supporting information), no matter what kind of light source is used for irradiation, the absorption spectra of TX-NHPIE-Cpe are almost unchanged with the extension of time, and the other three TX-NHPIEs have similar situations (Figs. S3-S5 in Supporting information), which can be attributed to the nature of TX itself and the cracking of active ester does not affect the UV absorption wavelength of TX-NHPIEs. The same photolysis phenomenon also occurred in the photolysis experiments of ITX, which is the expected result.

Enthalpies of the N–O bond cleavage process ($\Delta H_{\text{cleavage S1/T1}} = \text{BDE(N–O)} - E_{S1}/E_T$) from singlet excited state (S_1) or triplet excited state (T_1) were computed and could be applied for evaluating how favorably the cleavage reactions will take place. The N–O bond dissociation energies (BDE), singlet excited-state energies (E_{S1}) and triplet excited-state energies (E_{T1}) of TX-NHPIEs were confirmed by computations (Table S3 in Supporting information). In addition, possible pathways of bond cleavage at singlet state and triplet state have been described using TX-NHPIE-Cpe as the model (Fig. S7 in Supporting information). The E_{S1} was experimentally verified and values were calculated according to the equation $E = hc/\lambda$, where h is the Planck constant, c is the speed of light, and λ is the wavelength corresponding to the intersection of experimental absorption and fluorescence emission spectra (Fig. S8a in Supporting information). The E_{S1} measurements for the other TX-NHPIEs are shown in Fig. S9 (Supporting information). The free energy calculation of the reaction pathways of the cleavage process from the singlet state and from the triplet state indicate that the cleavage from the broken symmetry singlet state is energetically favorable. Besides, the fluorescence lifetime of TX-NHPIEs was measured (Figs. S8b and S10 in Supporting information). TX-NHPIEs have a short fluorescence lifetime, among them, the fluorescence lifetime of TX-NHPIE-Vi and TX-NHPIE-Cpe is only 3.28 ns and 3.30 ns. In other words, intersystem crossing process was not clearly observed. These experimental and computational results indicated that the cleavage might occur at singlet, though it would immediately lead to recombination of the radical pair. Further calculations is needed for more detailed explanations.

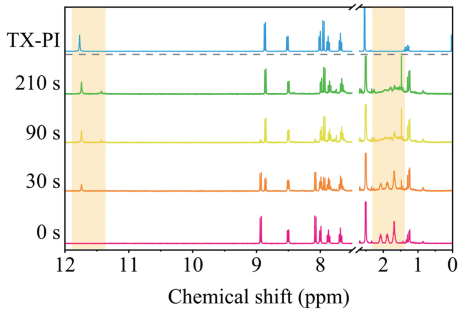

Fig. 3. Real-time ^{1}H NMR (400 MHz, DMSO–d_6) spectral changes of TX-NHPIE-Cpe irradiated by LED@405 nm under argon atmosphere and compared with TX-PI.

To investigate the decomposition mechanism of TX-NHPIEs, TX-NHPIE-Cpe was dissolved in DMSO–d_6 under an argon atmosphere and the solution was irradiated with LED@405 nm (Fig. 3). After 210 s of irradiation, the characteristic peaks of the cyclopentyl group of TX-NHPIE-Cpe (2.16, 1.88, and 1.68 ppm) gradually weakened to disappear completely. Meanwhile, the peaks at 11.7, 11.4 and 1.48 ppm gradually increase, which may be attributed to the N–H protons of precursor thioxanthone-based phthalimide (TX-PI), carboxylic acid protons and cyclopentane protons, respectively. The change in peak displacement of the aromatic region also proves the production of TX-PI. It is demonstrated that the N–O bond in TX-NHPIE breaks and undergoes a deacidification reaction to produce the corresponding alkyl radicals.

To verify the break of the N–O bond during the process of photopolymerization, further studies by decarboxylation and GC–MS experiments were conducted. The fading of the phenolphthalein solution in the right bottle indicates that TX-NHPIEs can produce CO_2 under light irradiation (Fig. S11 in Supporting information), which also illustrates the break of the N–O bond. This result was also confirmed in GC–MS experiments ($m/z = 281$: $C_{15}H_7NO_3S$, Fig. S12 in Supporting information).

ESR experiment was conducted for future insight into the photolysis mechanism. The solution of TX-NHPIE-Cpe was irradiated by LED@405 nm for 15 min. A free radical is observed to be captured by the *N*–*tert*–butyl–α-phenylnitrone (PBN) in Fig. S13 (Supporting information), with hyperfine coupling constants of $a_N = 14.65$ G and $a_H = 2.42$ G. According to the reference, this signal is the corresponding carbon-centered radical produced by TX-NHPIE-Cpe upon photolysis [45]. The experimental and calculated spectra of TX-NHPIE-Vi are shown in Fig. S14 (Supporting information).

Based on the results of photolysis, real-time ^{1}H NMR, ESR, decarboxylation, GC–MS, and computational experiments, the most plausible photoinitiation process mechanism was submitted

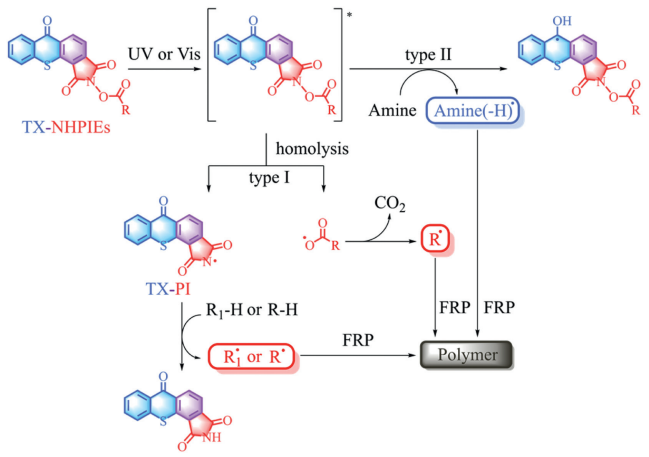

Scheme 1. Proposed mechanism of photoinduced radical generation.

(Scheme 1). TX-NHPIEs are conjugated by TX and NHPIE through a benzene ring. TX-NHPIEs absorb light energy and form an excited state, then there are two possible reaction pathways the excited TX-NHPIEs can choose. On the one hand, the excited TX-NHPIEs undergo homolysis cleavage resulting in the formation of thioxanthone-based phthalimide (TX-PI) radical and acyloxy radical (type I). Then, the acyloxy radical undergoes decarboxylation, removing CO_2 to form the corresponding reactive radical, thus inducing the monomer to undergo FRP. Meanwhile, TX-PI radical can abstract hydrogen atom from solvent or monomer to form reactive radicals for inducing FRP. On the other hand, TX-NHPIEs can act as type II PIs by reacting with amine through an electron transfer in order to generate reactive amine radical for inducing FRP.

The initiating activity of TX-NHPIEs and ITX for free radical polymerization was explored. The kinetic data indicated that TX-NHPIEs and ITX demonstrate excellent initiation efficiency for FRP as unimolecular PI under the irradiation of LED@365 nm and 405 nm, respectively (Figs. 4a, b, d and e). However, it is worth noting that the initiating activity of TX-NHPIEs is much higher than ITX, and ITX can hardly initiate the polymerization of tripropylene glycol diacrylate (TPGDA) and trimethylol propane triacrylate (TMPTA) as unimolecular PI under the irradiation of LED@450 nm (Figs. 4c and f), which is an innovative point designed in this work. Among the four synthesized TX-NHPIEs, TX-NHPIE-Cpe showed the highest initiation efficiency, and the order of initiation activity is as follows: TX-NHPIE-Cpe > TX-NHPIE-Cpr > TX-NHPIE-Vi > TX-NHPIE-Me.

On the other hand, when TX-NHPIEs and ITX were combined with hydrogen donor triethanolamine (TEOA) as type II PIs, both TX-NHPIEs and ITX exhibited high initiation efficiency under LED@365 nm and 405 nm light irradiation, which is similar to their use as type I PIs. Under the irradiation of LED@450 nm light source, the initiation rate of ITX increased, but it is still lower than the designed TX-NHPIEs in this work. As shown in Figs. S15c and f (Supporting information), the initiation rate of both TPGDA and TMPTA is very slow in the first 50 s. This once again proves the importance of the PI designed in this work for initiating monomer polymerization under LED@ 450 nm light source irradiation.

Thermal and storage stability are significant indexes to evaluate a PI. Thermal gravimetric analysis (TGA) and differential scanning calorimetry (DSC) experiments suggest that TX-NHPIEs have excellent thermal stability (Fig. S16a in Supporting information) and storage stability (Fig. S16b in Supporting information), which can meet the requirements of industrial applications. It should be noted that the onset temperature of thermal polymerization of TMPTA is 132 °C [46], when adding TX-NHPIEs in TMPTA, the polymerization temperature of TMPTA increased to 177–181 °C (Table S4 in Supporting information).

The mechanical properties and thermal stability energy of coatings, cured by the same photosensitive resin formulations initiated by four TX-NHPIEs and ITX as PI respectively, were determined. From Fig. S17 and Table S5 (Supporting information), we can see tensile strength, Young's modulus, glass transition temperature of the coatings cured by the formulations containing TX-NHPIEs are higher than the coatings cured by the formulations

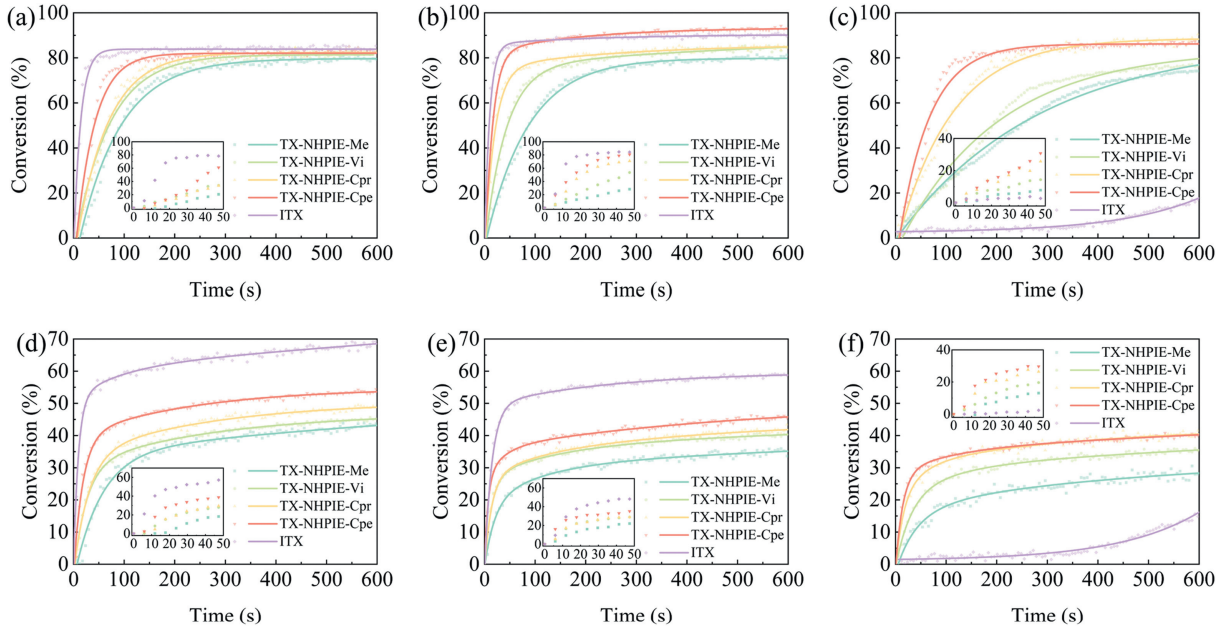

Fig. 4. Photopolymerization profiles of TPGDA (a-c) and TMPTA (d-f) in the presence of PIs (1.3×10^{-5} mol/g) under LED@ 365 nm (a, d), LED@405 nm (b, e), LED@450 nm (c, f) irradiation.

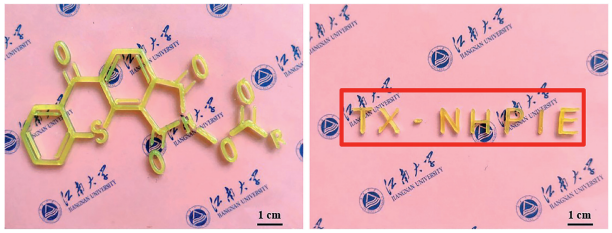

Fig. 5. 3D printed the molecular structure formula and letters of TX-NHPIE.

containing ITX. This is because at the same molar ratio as ITX, TX-NHPIEs can generate more active free radicals to initiate polymerization, resulting in an increased cross-linking of the system. The mechanical properties and thermal stability of the coatings, cured by the formulations initiated by four TX-NHPIEs, are improved due to high crosslinking. Moreover, the coatings cured by the formulations initiated by TX-NHPIE-Vi have the lowest elongation at break, which may be due to the fact that TX-NHPIE-Vi has unsaturated groups and can cross-link with the resin, which further increases the crosslinking density of the system. Compared with a commercialized ITX initiating system, TX-NHPIEs are beneficial for improving the mechanical properties and thermal stability of the bisphenol A epoxy acrylate (RY1101) : isobornyl acrylate (IBOA) = 1 : 1 resin system.

Application of TX-NHPIE-Cpe (1.3×10^{-5} mol/g) for photo-direct ink writing (DIW) (Fig. 5). The ink is adjusted to have proper rheological properties to provide excellent shape retention ability, and ink is pressurized by extruding the ink and printing with a three-axis *X-Y-Z* platform movement. After printing, rapid curing is carried out using a LED@450 nm light source radiation. Under the condition of ensuring the resolution of the final objects, the molecular structure formula (105 mm × 50.7 mm × 2 mm) and letters (1.5–9.3 mm × 10 mm × 2 mm) of TX-NHPIE are printed at a fast printing speed (10 mm/s).

In conclusion, four kinds of TX-NHPIEs, as efficient UV–vis PIs, were synthesized and characterized, and their applications in coatings and 3D printing were investigated thoroughly. Compared with the commercialized ITX, TX-NHPIEs have longer UV absorption (red shift to 480 nm) and demonstrate sterling initiating efficiency for FRP under LED@450 nm light irradiation. The initiation mechanism of TX-NHPIEs was proposed based on real-time ^{1}H NMR, ESR, decarboxylation and GC–MS experiments. Meanwhile, the above experimental results and kinetic experiments prove that as type I PIs, TX-NHPIEs absorb one photon can produce two active radicals, which break the limitation of traditional PIs that can only produce one active radical when absorbing one photon. Furthermore, kinetic experiments evidence that TX-NHPIEs also have good initiating activity as type II PIs. Moreover, TX-NHPIEs also have good thermal stability, it is worth noting that when TX-NHPIEs were added to TMPTA, the onset temperature of TMPTA will increase. In summary, TX-NHPIE PIs can be used as type I/II PIs, exhibiting efficient photoinitiation ability under visible light initiation and excellent thermal stability, demonstrating enormous commercial potential.

Declaration of competing interest

The authors declare that they have no known competing financial interests or personal relationships that could have appeared to influence the work reported in this paper.

Acknowledgments

The authors acknowledge the financial support by the National Natural Science Foundation of China (Nos. 22301107, 52373057) and the Nature Science Foundation of Jiangsu Province (No. BK20200610) and the Fundamental Research Funds for the Central Universities (No. JUSRP122021). Jiangsu Province "Innovation and Entrepreneurship Doctor" Talent Plan (No. JSSCBS20221053) also provided support. The authors express their gratitude to high-performance computing cluster platform of the School of Biotechnology in Jiangnan University.

Supplementary materials

Supplementary material associated with this article can be found, in the online version, at doi:10.1016/j.cclet.2024.109573.

References

[1] C. Wu, N. Corrigan, C.H. Lim, et al., Chem. Rev. 122 (2022) 5476–5518.
[2] F. Jasinski, P.B. Zetterlund, A.M. Braun, A. Chemtob, Prog. Polym. Sci. 84 (2018) 47–88.
[3] N. Corrigan, J. Yeow, P. Judzewitsch, J. Xu, C. Boyer, Angew. Chem. Int. Ed. 58 (2019) 5170–5189.
[4] L. Pierau, C. Elian, J. Akimoto, et al., Prog. Polym. Sci. 127 (2022) 101517.
[5] C. Li, B. Lee, C. Wang, et al., Mater. Horiz. 9 (2022) 452–461.
[6] Y. Sanai, T. Ninomiya, K. Arimitsu, Prog. Org. Coat. 151 (2021) 106038.
[7] J. Tong, Y. Mao, J. Pi, J. Luo, R. Liu, Prog. Org. Coat. 177 (2023) 107438.
[8] S. Baek, H.W. Ban, S. Jeong, et al., Nat. Commun. 13 (2022) 5262.
[9] S.C. Gauci, A. Vranic, E. Blasco, et al., Adv. Mater. 36 (2024) 2306468.
[10] T. Gerges, V. Semet, P. Lombard, B. Allard, M. Cabrera, Addit. Manuf. 73 (2023) 103673.
[11] P. Wen, P. Lu, X. Shi, et al., Adv. Energy Mater. 11 (2021) 2002930.
[12] H.E. Pudavar, M.P. Joshi, P.N. Prasad, B.A. Reinhardt, Appl. Phys. Lett. 74 (1999) 1338–1340.
[13] G. Chen, Z. Zhang, W. Zhang, et al., Mater. Horiz. 8 (2021) 2018–2024.
[14] F. Bella, G. Griffini, J.P. Correa-Baena, et al., Science 354 (2016) 203–206.
[15] J.R. Tumbleston, D. Shirvanyants, N. Ermoshkin, et al., Science 347 (2015) 1349–1352.
[16] Y. Zhao, J. Zhu, W. He, et al., Nat. Commun. 14 (2023) 2381.
[17] Y. Bao, Macromol. Rapid Commun. 43 (2022) 2200202.
[18] Y. Bao, N. Paunović, J.C. Leroux, Adv. Funct. Mater. 32 (2022) 2109864.
[19] J. Yang, Y. Cheng, X. Gong, et al., Chin. Chem. Lett. 33 (2022) 2231–2242.
[20] A.A. Pérez-Mondragón, C.E. Cuevas-Suárez, J.A. González-López, N. Trejo-Carbajal, A.M. Herrera-González, J. Photochem. Photobiol. A 403 (2020) 112844.
[21] H.F. Gruber, Prog. Polym. Sci. 17 (1992) 953–1044.
[22] A. Sun, X. He, X. Ji, et al., Chin. Chem. Lett. 32 (2021) 2117–2126.
[23] F. Dumur, Eur. Polym. J. 187 (2023) 111883.
[24] P. Xiao, J. Zhang, F. Dumur, et al., Prog. Polym. Sci. 41 (2015) 32–66.
[25] R. Zhou, H. Pan, D. Wan, J.P. Malval, M. Jin, Prog. Org. Coat. 157 (2021) 106306.
[26] P. Garra, J.P. Fouassier, S. Lakhdar, Y. Yagci, J. Lalevée, Prog. Polym. Sci. 107 (2020) 101277.
[27] J. Shao, Y. Huang, Q. Fan, Polym. Chem. 5 (2014) 4195–4210.
[28] S. Liu, T. Borjigin, M. Schmitt, et al., Polymers 15 (2023) 342.
[29] C. Elian, N. Sanosa, N. Bogliotti, et al., Polym. Chem. 14 (2023) 3262–3269.
[30] F. Hammoud, A. Hijazi, M. Schmitt, F. Dumur, J. Lalevée, Eur. Polym. J. 188 (2023) 111901.
[31] F.D. Saeva, D.T. Breslin, P.A. Martic, J. Am. Chem. Soc. 111 (1989) 1328–1330.
[32] Z. Li, X. Zou, G. Zhu, X. Liu, R. Liu, ACS Appl. Mater. Interfaces 10 (2018) 16113–16123.
[33] S. Liu, N. Giacoletto, M. Schmitt, et al., Macromolecules 55 (2022) 2475–2485.
[34] S. Liu, N. Giacoletto, B. Graff, et al., Mater. Today Chem. 26 (2022) 101137.
[35] T. Patra, S. Mukherjee, J. Ma, F. Strieth-Kalthoff, F. Glorius, Angew. Chem. Int. Ed. 58 (2019) 10514–10520.
[36] S.K. Parida, T. Mandal, S. Das, et al., ACS Catal. 11 (2021) 1640–1683.
[37] K. Okada, K. Okamoto, M. Oda, J. Am. Chem. Soc. 110 (1988) 8736–8738.
[38] C.M. Chan, Q. Xing, Y.C. Chow, S.F. Hung, W.Y. Yu, Org. Lett. 21 (2019) 8037–8043.
[39] S. Shibutani, T. Kodo, M. Takeda, et al., J. Am. Chem. Soc. 142 (2020) 1211–1216.
[40] S. Dadashi-Silab, C. Aydogan, Y. Yagci, Polym. Chem. 6 (2015) 6595–6615.
[41] T. Li, Z. Su, H. Xu, et al., Chin. Chem. Lett. 29 (2018) 451–455.
[42] M.H. He, R.X. Xu, G.X. Chen, Z.H. Zeng, J.W. Yang, Chin. Chem. Lett. 25 (2014) 1445–1448.
[43] T. Lu, F. Chen, J. Comput. Chem. 33 (2012) 580–592.
[44] P. Xiao, F. Dumur, B. Graff, et al., Macromolecules 47 (2014) 973–978.
[45] V.E. Kholmogorov, Russ. Chem. Rev. 37 (1968) 628.
[46] D. Xu, X. Zou, Y. Zhu, et al., Prog. Org. Coat. 166 (2022) 106772.